ELSEVIER

Materials Science and Engineering A 466 (2007) 38–46

MATERIALS SCIENCE & ENGINEERING A

www.elsevier.com/locate/msea

Compressive and fatigue damage behavior of commercially pure zinc

H. Li [a,b], Q.Q. Duan [a], X.W. Li [b], Z.F. Zhang [a,*]

[a] *Shenyang National Laboratory for Materials Science, Institute of Metal Research, Chinese Academy of Sciences, Shenyang 110016, PR China*
[b] *Institute of Materials Physics & Chemistry, College of Sceinces, P.O. Box 104, Northeastern University, Shenyang 110004, PR China*

Received 3 January 2007; received in revised form 6 February 2007; accepted 19 February 2007

Abstract

The deformation and damage behaviors of commercially pure zinc were investigated under compression and cyclic compression–compression loadings. After the tests above, the surface deformation morphologies and fatigue crack initiation of all the deformed samples were carefully observed by optical microscope (OM) and scanning electron microscope (SEM). Compressive tests on the commercially pure zinc indicated that the deformation and damage mechanisms are slightly different from those under cyclic compression–compression loading. The main deformation and damage mechanisms consist of slipping, twinning, secondary twinning, kinking, cracking along grain boundary and twin boundary under different loadings. Based on the experimental results, the compressive and fatigue damage mechanisms were discussed.

Keywords: Commercially pure zinc; Compression; Fatigue; Slip bands; Deformation twins; Grain boundary

1. Introduction

It is well known that the main plastic deformation mechanisms of those hexagonal close-packed (HCP) metals are twinning and slipping. Because HCP metals only have a few slip systems, sometimes twinning often plays a more important role than slipping for the plastic deformation. In metal family, there are many HCP metals, for example, Ti, Mg, Be, Zn, Re, Zr, etc. On one hand, it is noted that the ratio *c*/*a* is a very important parameter for the plastic deformation modes of those HCP metals. For example, the HCP metals like Re, Zr and Ti with *c*/*a* less than 1.63 often have a good plasticity and can deform via twinning either under tensile or under compressive loading [1]. However, for those HCP metals like Zn and Be with *c*/*a* larger than 1.63, twinning ($\{1\,0\,\bar{1}\,2\}[1\,0\,\bar{1}\,\bar{1}]$) can be activated mainly under compression, and they exhibit a poor plasticity when subjected to tensile load [1]. On the other hand, it can be easily calculated that the maximum plasticity provided by twinning deformation could only reach about 7% [2,3], which is much smaller than that via slip deformation. So the significance of twinning is suggested to be able to change the orientations of the neighboring grains and induce new slip deformation for those slip systems with smaller Schmid factor [4].

Recently, the plastic deformation mechanisms of HCP metals, such as Ti [5–15] and Zr [16–18] with a *c*/*a* value less than 1.63, were widely investigated. It is found that different deformation mechanisms may take effect in these HCP metals with the changes of temperature, purity, loading mode, etc. In contrast, few people have thoroughly investigated the plastic deformation mechanism of pure zinc, which has a larger *c*/*a* of 1.856 [3,19–23]. In particular, to the best our knowledge, there is few report about both the compressive and fatigue tests on pure zinc. As is well known, zinc, as one of typical HCP metals, has a larger *c*/*a* than those of Ti and Zr, it is thus believed that there must be some special properties and different deformation and damage mechanisms during plastic deformation. The main objective of the current paper is to further reveal the fundamental plastic deformation and damage mechanisms of pure zinc under compression and cyclic compression–compression loadings. It is expected that the current research on pure zinc can provide additional information for comprehensively understanding the deformation and damage mechanisms of HCP metals.

2. Experimental procedures

The experimental specimens are commercially pure zinc of 99.995% purity made by casting method. The average grain size was measured to be about 1–3 mm by optical microscope (OM). Such coarse grain size is beneficial to reveal the local defor-

* Corresponding author. Tel.: +86 24 23971043; fax: +86 24 23891320.
E-mail address: zhfzhang@imr.ac.cn (Z.F. Zhang).

0921-5093/$ – see front matter © 2007 Elsevier B.V. All rights reserved.
doi:10.1016/j.msea.2007.02.062

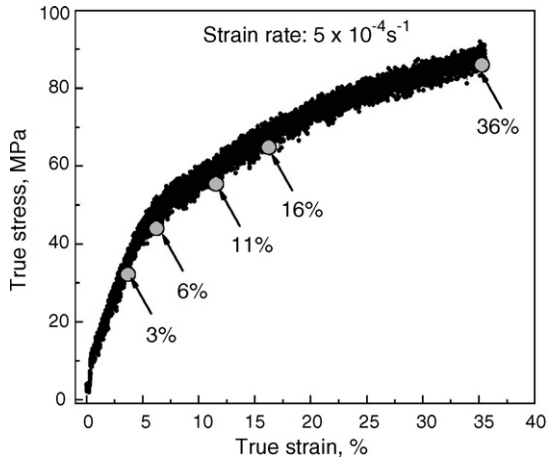

Fig. 1. True stress–strain curve of compressive specimens under different strains at a strain rate of $5 \times 10^{-4}\ s^{-1}$.

mation and damage mechanisms within individual grain. The dimension of all the specimens for compressive and fatigue tests is 4 mm × 4 mm × 8 mm. Before tests, all the specimens were mechanically polished for surface observations. The compression and cyclic compression–compression tests were performed with a MTS810 fatigue testing machine at room temperature. For the compression tests, the specimens were deformed at a strain rate of about $5 \times 10^{-4}\ s^{-1}$ up to different strains of 3, 6, 11, 16 and 36%, respectively. The stress controlled cyclic compression–compression tests were carried out at different stress amplitudes of 22.5, 25 and 27.5 MPa at a frequency of 1 Hz. The wave shape is sine wave, and all the samples were cyclically compressed for 200 cycles. The minimum stress is 5 MPa for all the fatigued specimens, while the maximum stresses are 50, 55 and 60 MPa, respectively. After the mechanical tests above, all the specimens were carefully observed by optical microscope and scanning electron microscope (SEM) to reveal the surface deformation and damage morphologies, as well as the nucleation of fatigue cracks.

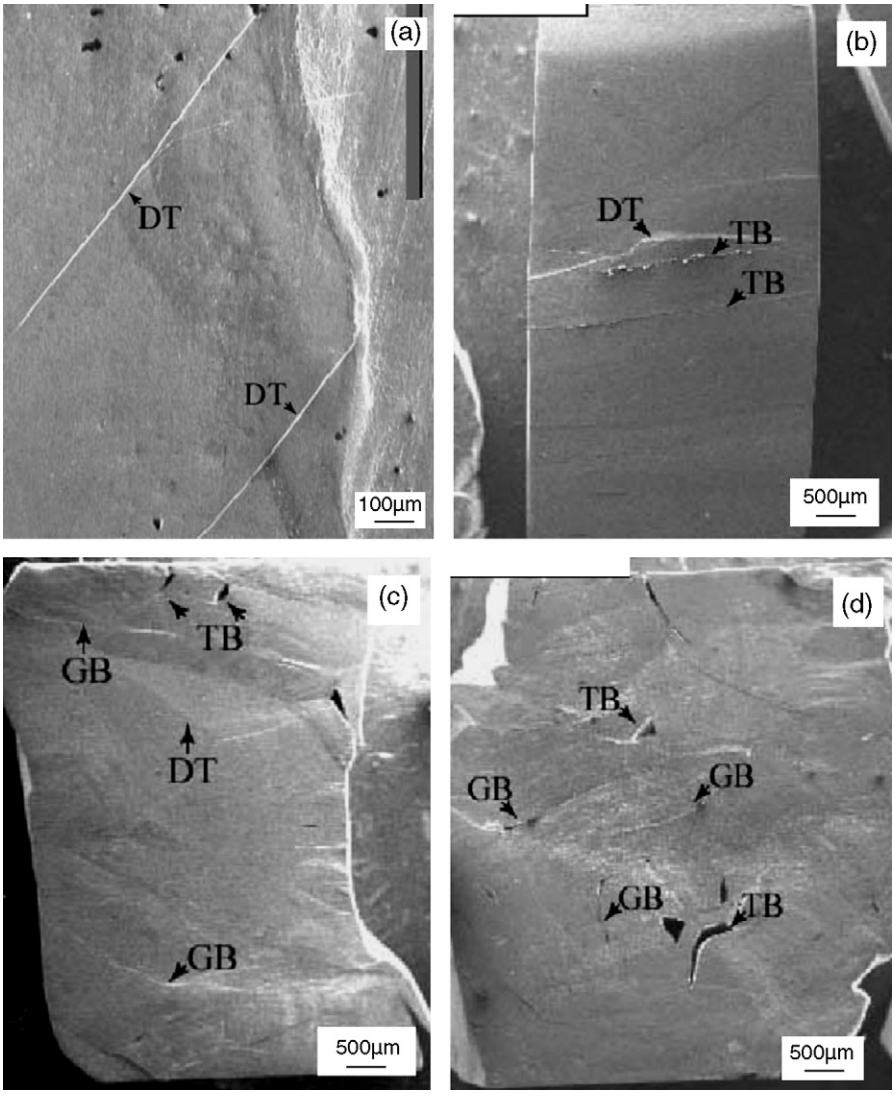

Fig. 2. Macro-scale compressive deformation and damage morphologies of polycrystalline Zn specimens at different strains: (a) 3%; (b) 6%; (c) 16%; (d) 36%. DT, deformation twin; TB, twin boundary; GB, grain boundary.

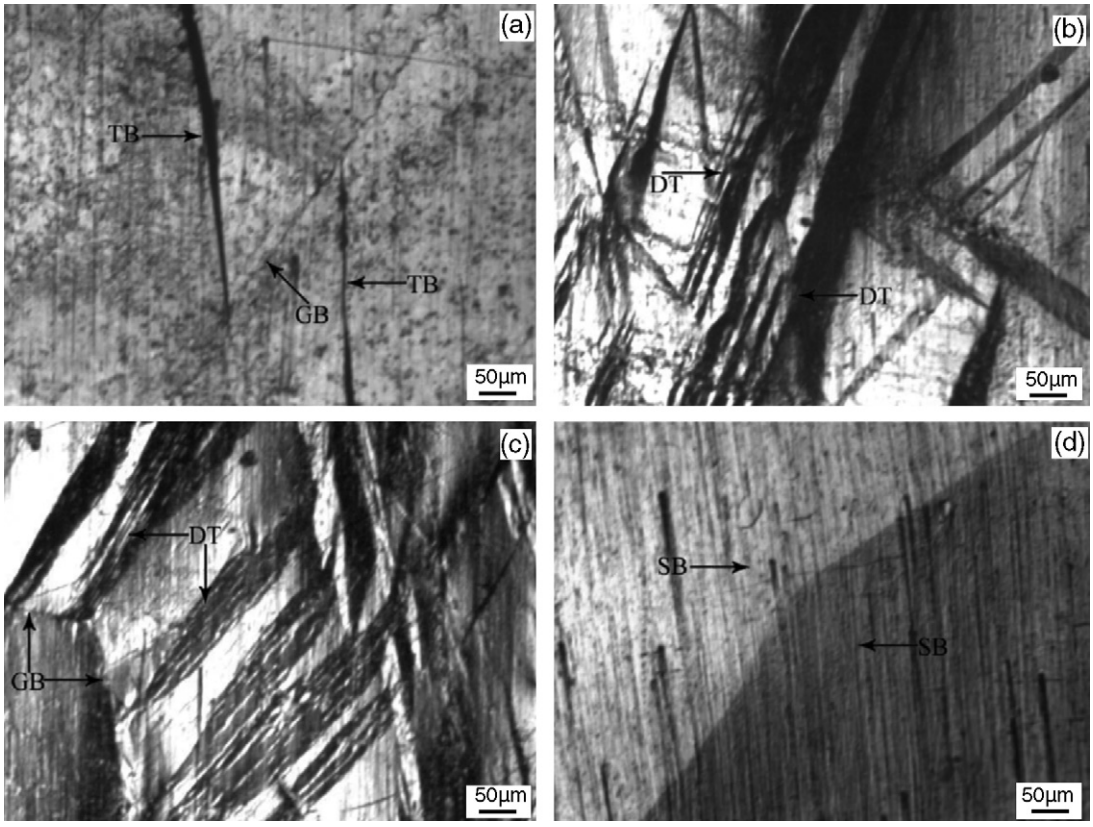

Fig. 3. Micro-scale deformation and damage morphologies of polycrystalline Zn specimens at a strain of 3%. (a) Close to grain boundary, (b) interior of grain, (c) close to grain boundary, (d) close to edge of sample. SB, slip band.

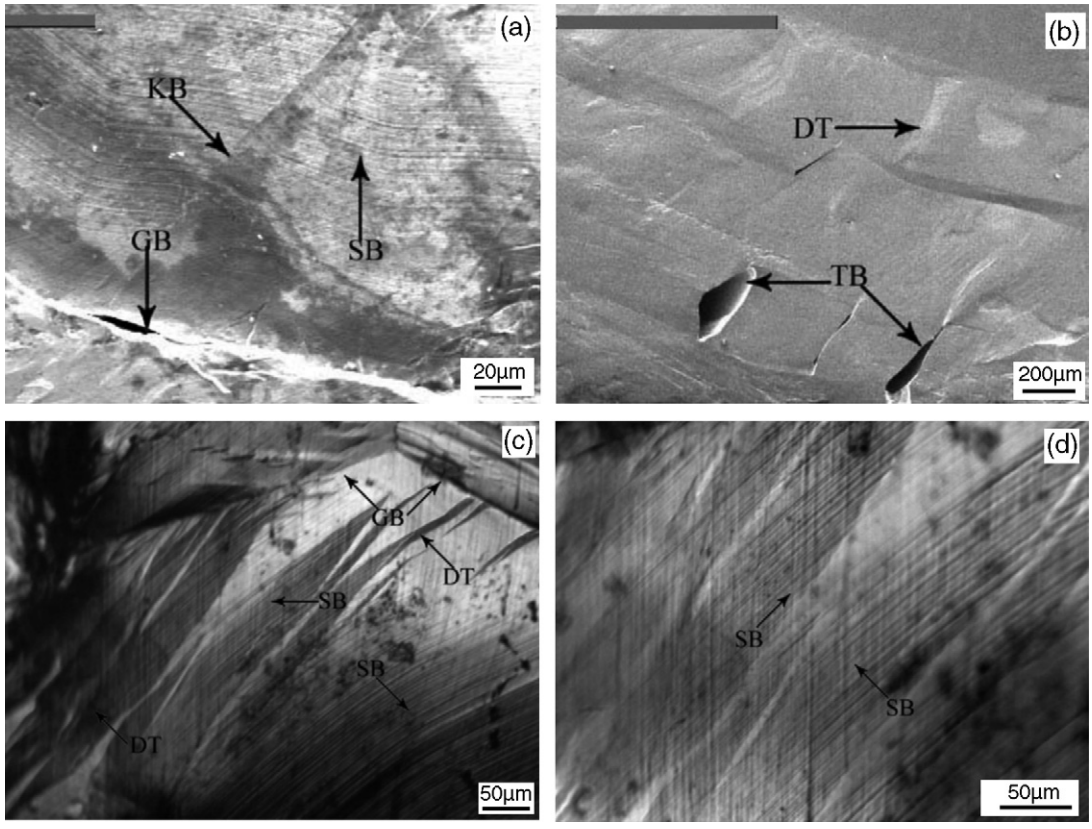

Fig. 4. Micro-scale deformation and damage morphologies of polycrystalline Zn specimens at a strain of 6%. (a) Close to grain boundary, (b) interior of grain, (c) close to grain boundary, (d) interior of grain. KB, kink band.

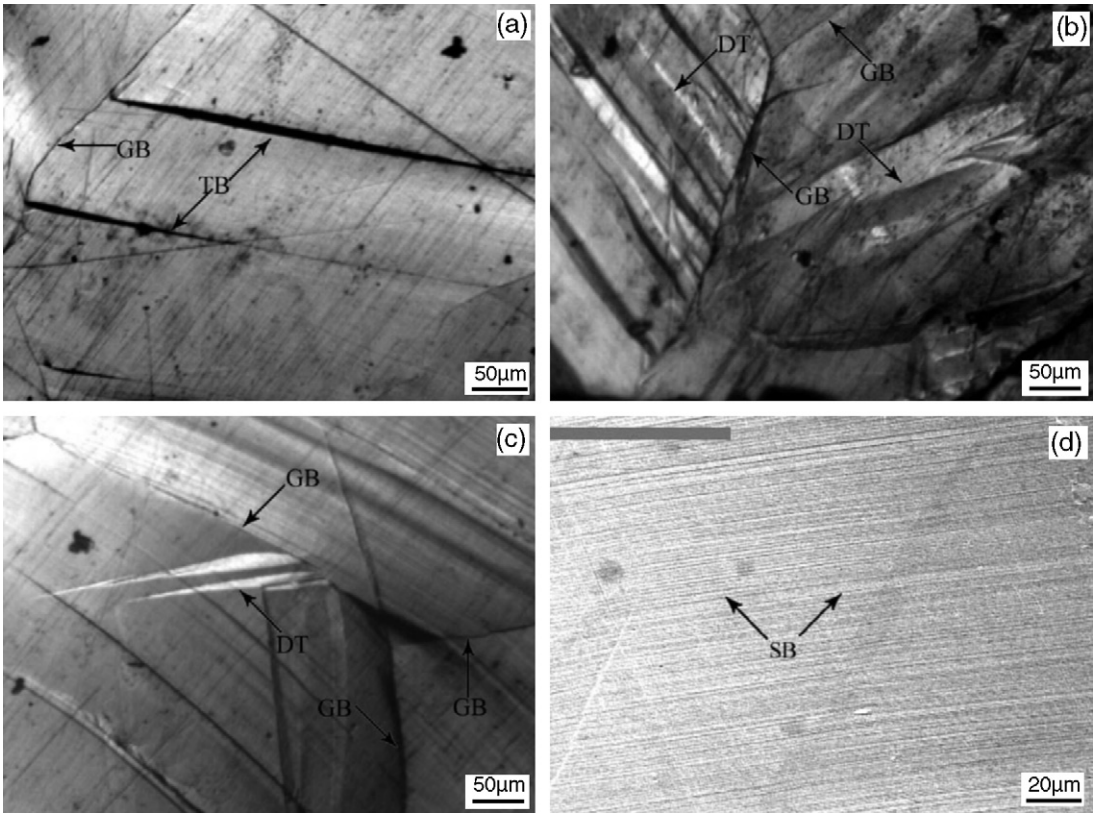

Fig. 5. Micro-scale deformation and damage morphologies of polycrystalline Zn specimens at a strain of 16%. (a) Close to grain boundary, (b) close to grain boundary, (c) close to grain boundary, (d) interior of grain.

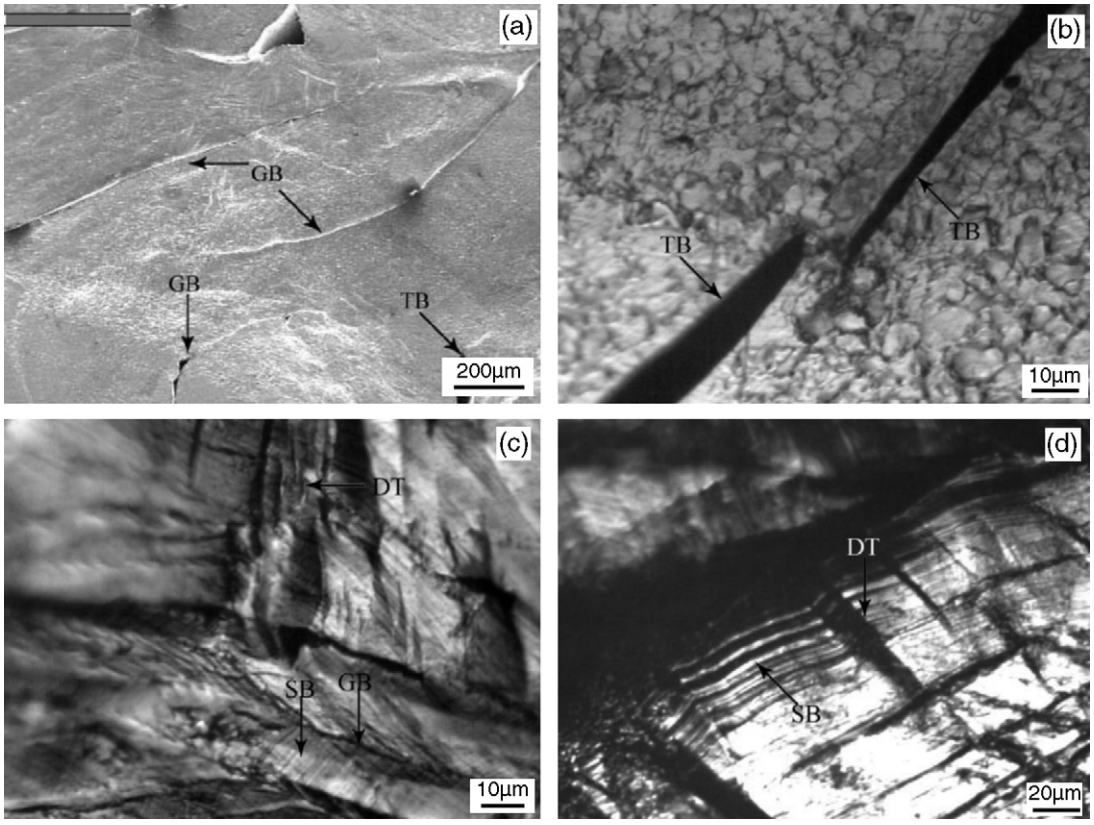

Fig. 6. Micro-scale deformation and damage morphologies of polycrystalline Zn specimens at a strain of 36%. (a) Close to grain boundary, (b) interior of grain, (c) close to grain boundary, (d) interior of grain.

3. Results and discussion

3.1. Compression stress–strain curve

Fig. 1 shows the compressive true stress–strain curve of the polycrystalline Zn specimen at a strain rate of about $5 \times 10^{-4}\,s^{-1}$. The yield stress of the specimens is about 13.8 MPa and the maximum compressive strain was applied to 36%. It can be seen that, after yielding, the polycrystalline Zn displays obvious work-hardening behavior up to a stress level of ~90 MPa, which is lower than the stress level of the pure zinc with a fine grain size of 40–78 μm by Chmelik et al. [22]. Meanwhile, it is noted that there exist abundant serrated flow features during plastic deformation, which is associated with the formation of deformation twin (DT) after each load drop, and some slip systems might take active, leading to stress rise [19]. For better understanding of the plastic deformation mechanism of polycrystalline Zn, several other specimens were prepared and compressed to different strains of 3, 6, 11 and 16%, respectively, as marked in the compressive curve. Afterwards, all the compressed specimens above were observed by OM and SEM to show the deformation morphology and evolution of slip bands and deformation twins. It is found that those serrated flow features are mainly attributed to the formation and evolution of deformation twins and local cracks as well as the interactions between slip bands and deformation twins, which will be discussed in the following section.

3.2. Compressive deformation and damage features

Fig. 2(a–d) shows the macro-scale compressive deformation and damage morphologies of polycrystalline Zn specimens under different strains of 3, 6, 16 and 36%. It can be seen that an increase in the applied strain would obviously aggravate deformation and damage. For examples, at low strains of 3 and 6%, there are only few local deformation twins activated on the specimen surfaces (see Fig. 2(a and b)). As the compressive strain increases, the deformation and damage behave rather severely, and the specimens become bended at high strains of 16 and 36%, as shown in Fig. 2(c and d). This indicates that the polycrystalline Zn can accommodate relatively high compressive strain without obvious failure. Meanwhile, several local cracks can be clearly seen on the specimen surface, as indicated by the arrows in Fig. 2(c and d). It is believed that the deformation and damage mechanisms at low and high strain levels must be quite different and the evolution of deformation and damage will be revealed as below in detail.

At the lowest compressive strain of 3%, the main deformation and damage features are shown in Fig. 3(a–d). At this strain level, the specimen surfaces were not severely damaged (Fig. 2(a)). However, $\{1\,0\,\bar{1}\,2\}[1\,0\,\bar{1}\,\bar{1}]$ deformation twins took place more easily in compression than in tension [1], so the deformation twins are found to be activated quite easily even at a small compressive strain of 3%. Because the sharp edge of a lenticular deformation twin lamella will cause a stress concentration as a crack [3,19], a limited number of cracks have formed along some twin boundaries (TBs). One can see grain boundaries (GBs)

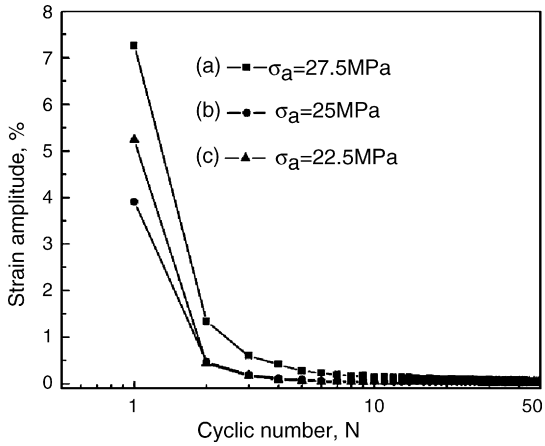

Fig. 7. Strain amplitude vs. cyclic number curves under different stress amplitudes.

clearly on the surface as indicated by the arrows in Fig. 3(a and c). Because the activation of deformation twins requires a lower applied stress than that for slip deformation, some deformation twins firstly formed on the surface of specimens (Fig. 3(b and c)), while slip bands (SBs) formed only at the edges of specimens (Fig. 3(d)).

When the strain increases to 6%, the main deformation and damage mechanisms are basically similar to the above one, but more cracks initiated, especially at grain boundaries (Fig. 4(a and c)). Under these circumstances, twin boundary cracks were formed more than those found in the above specimen (Fig. 4(b)). Meanwhile, more slip bands can be observed (Fig. 4(a, c and d)), and two slip systems may take active at the same area (Fig. 4(d)). Those slip bands may be basal and secondary pyramidal slip systems, also observed by Bell and Cahn [19] under tensile test. More deformation twins were activated (Fig. 4(b and c)), and some kinking bands (KBs) initiated at local area of the specimen (Fig. 4(a)).

With increasing the strain to 16%, in addition to slip bands, deformation twins and kinking bands were found, as shown in Fig. 5. Besides, there are more twin boundary cracks than grain boundary cracks, as shown in Fig. 5(a and c). But the main plastic deformation mechanisms are still twining and slipping.

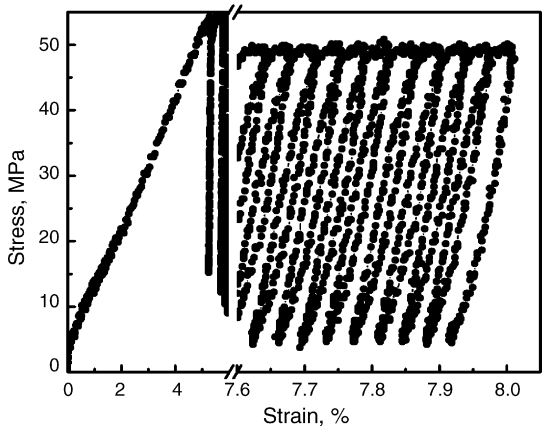

Fig. 8. Typical stress–strain curve of fatigue specimens.

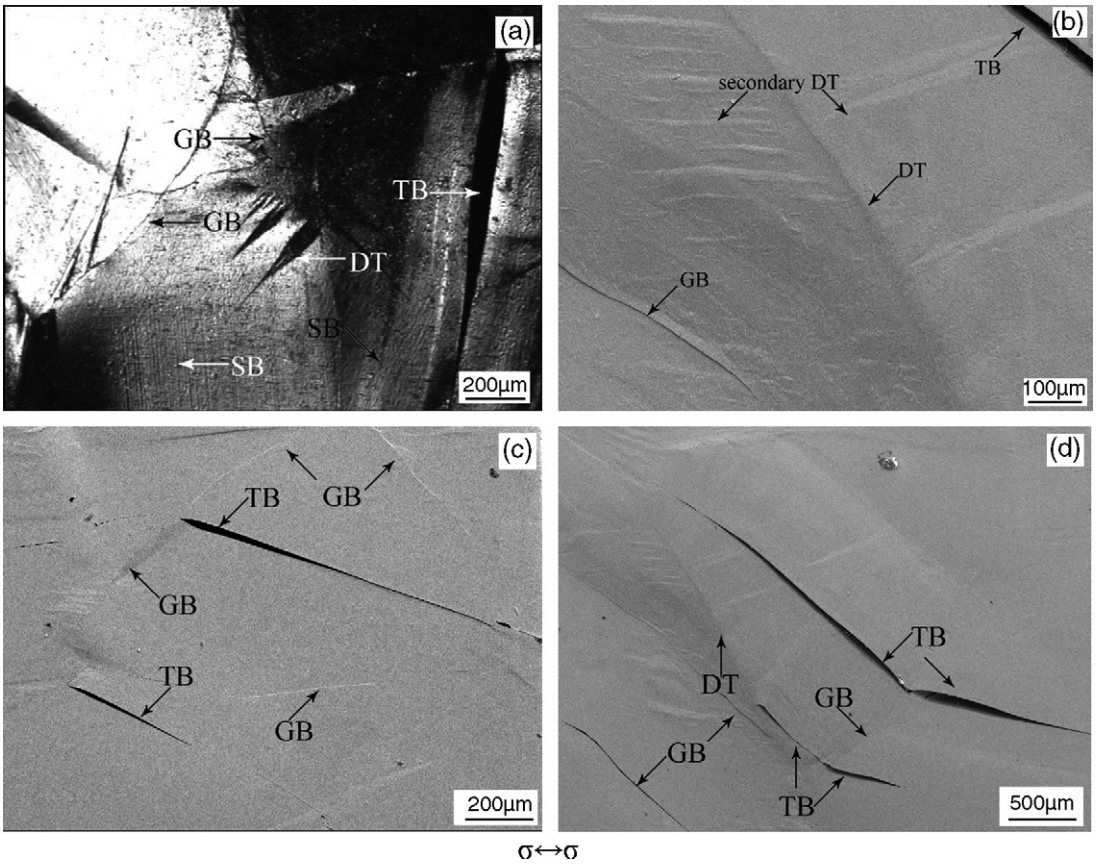

Fig. 9. Micro-scale deformation and damage morphologies of fatigue specimens at stress amplitude 22.5 MPa for 200 cycles.

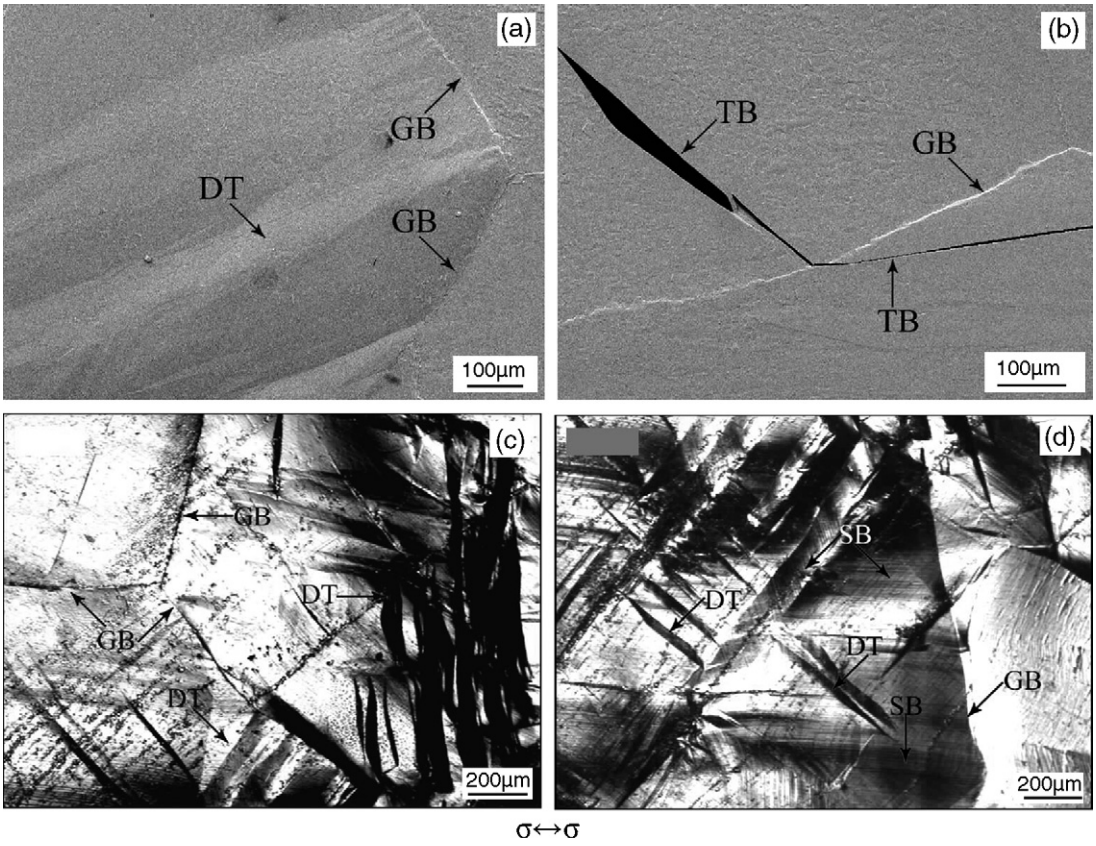

Fig. 10. Micro-scale deformation and damage morphologies of fatigue specimens at stress amplitude 25 MPa for 200 cycles.

As the strain was increased to 36%, the specimen was damaged so severely that one can hardly distinguish the deformation and damage mechanisms, as shown in Fig. 6(a–d). The specimen has formed somewhat larger cracks (Fig. 6(a and b)), whose main mechanisms are twin boundary cracks, because grain boundary cracks only relax a little plastic strain. The main mechanism of plastic deformation is still based on twinning (Fig. 6(c and d)), and more coarse slip bands were formed (see Fig. 6(d)). In particular, there exit strong interactions among deformation twins, slip bands and grain boundaries (see Fig. 6(c)).

From the observations in Figs. 2–6, one can realize that the main crack mechanism is cracking at grain boundaries at low strains. But, when the strain becomes higher, the dominant damage mechanism is switching to cracking at twin boundaries. The main plastic deformation mechanisms are slipping, twinning as well as kinking as observed by Chmelik et al. [22] in the polycrystalline Zn with coarse grain size under tensile test. Two slip systems can take active at the same area, and secondary deformation twins can be stimulated within the primary deformation twins. Besides, one can also observe some kinking bands only at local areas of the surface. Grain boundaries, as a kind of deformation impediment, can terminate the growth of deformation twins and slip bands, thus deformation twins cannot grow from one grain to another one; grain boundaries can terminate twin boundary cracks as well. The deformation and damage modes will be further summarized later.

3.3. Cyclic compression–compression curves

Fig. 7 gives the strain response curves with increasing cyclic number for the polycrystalline Zn specimens under different cyclic stress amplitudes (σ_a). It can be seen that the strain decreased rapidly at the beginning cycles and became stale when the cyclic number is over 10. Fig. 8 demonstrates the curves of the strain amplitude versus cyclic number under cyclic compression–compression fatigue experiments at all the applied stress amplitudes. The strain amplitude decreased gradually as the cyclic number increased, and came to a constant value quickly. This indicates that the polycrystalline Zn displayed significant cyclic hardening at the initial cycles and became cyclic saturation soon, and it is probably due to interference with pyramid slip by slip on a secondary pyramidal plane [19]. After some cycles, even when the stress amplitude is very high, there is no obvious difference among these three curves, but their hardening rates have a little bit different.

3.4. Cyclic deformation and damage features

Figs. 9–11 give the macro-scale surface deformation and damage morphologies of the fatigue specimens at different stress amplitudes of 22.5, 25 and 27.5 MPa, respectively. One can see that all the three specimens are damaged severely, but they can display good plasticity without failure, which can be attributed to the formation of massive deformation twins, kinking and

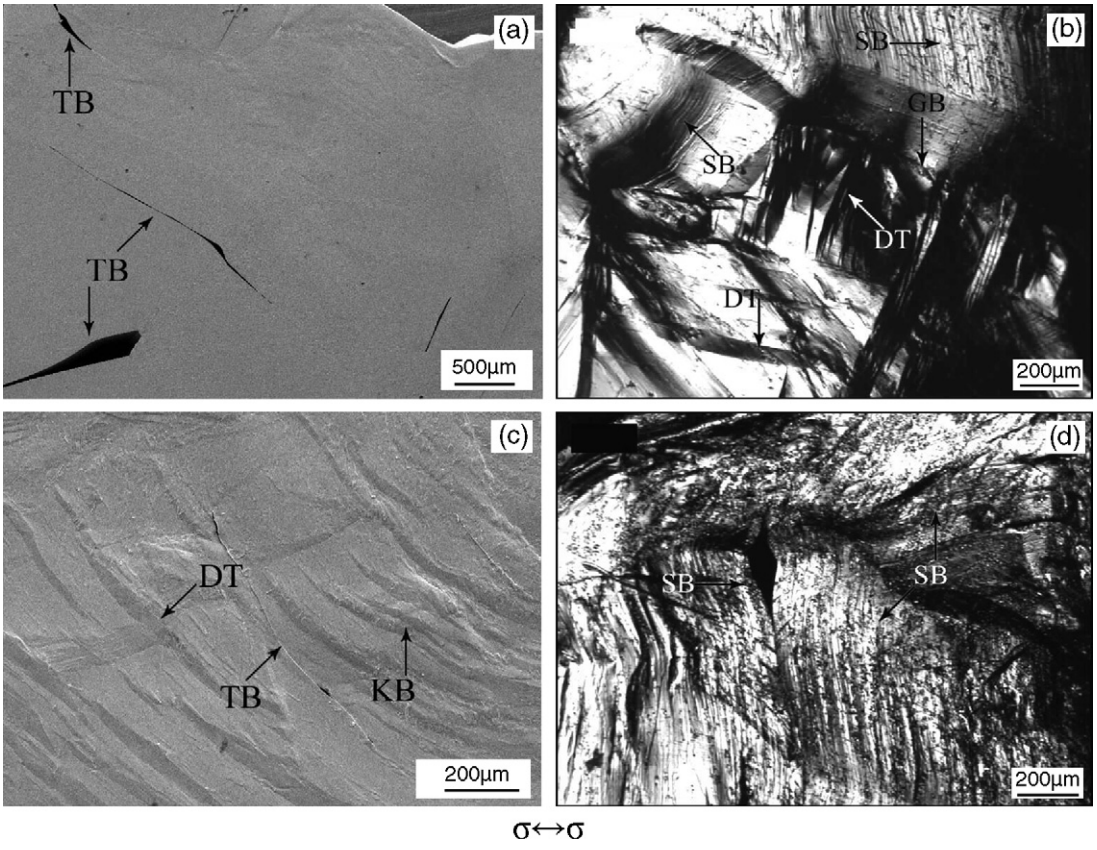

Fig. 11. Micro-scale deformation and damage morphologies of fatigue specimens at stress amplitude 27.5 MPa for 200 cycles.

slip bands. All of those deformation mechanisms should associated with the formation of secondary pyramidal slip [24] and $\{1\,0\,\bar{1}\,2\}[1\,0\,\bar{1}\,\bar{1}]$ twinning [1] more easily in compression than in tension. The main deformation and damage mechanisms are similar to those with the unidirectionally compressed specimens, but they also have some different characters, and it will be revealed as below in detail.

Firstly, one can see that the surfaces were not damaged very obviously from Fig. 9, which gives morphologies of the specimen fatigued at the lowest stress amplitude of 22.5 MPa. The main plastic deformation mechanisms are twinning (Fig. 9(a–d)), slipping (Fig. 9(a)), and some secondary twins within the coarse deformation twins (Fig. 9(b and d)). The main damage mechanisms are fatigue cracking at twin boundaries and grain boundaries (Fig. 9(a–d)). Grain boundaries can terminate the growth of deformation twins and twin boundary cracks (Fig. 9(a and c)). But if the applied stress concentrates somewhere, some twin boundary cracks can also transfer through the grain boundary and change their directions, and then they have a suitable direction to grow much larger (Fig. 9(d)).

As the stress amplitude increases to 25 MPa, the main deformation and damage mechanisms do not change much (Fig. 10(a and b)). One can observe some complex deformation twins and slip bands, which have complex interactions (Fig. 10(c and d)).

At a stress amplitude of 27.5 MPa, the deformation and damage mechanisms are still similar to the above two specimens (Fig. 11(a and b)). But the specimen has large cracks (Fig. 11(a and b)) and can accommodate high accumulated plastic deformation (Fig. 11(b)). Some kinking bands were observed to initiate and slip bands and deformation twins distorted at the kinked area (Fig. 11(c and d)).

From the observations above it is strongly suggested that under cyclic compression–compression loading, the main plastic deformation mechanisms are twinning, slipping, kinking, too. Twinning and slipping mechanisms and their interactions with grain boundaries are similar to that under unidirectionally compressive tests. The main crack mechanisms are fatigue cracking at twin boundaries and grain boundaries as well as cracking along slip bands. Grain boundaries can terminate slip band cracks, but sometimes cannot terminate twin boundary cracks. Therefore, the main deformation and damage mechanisms of commercially pure zinc under unidirectional compression and cyclic compression–compression loadings can be well summarized in Fig. 12.

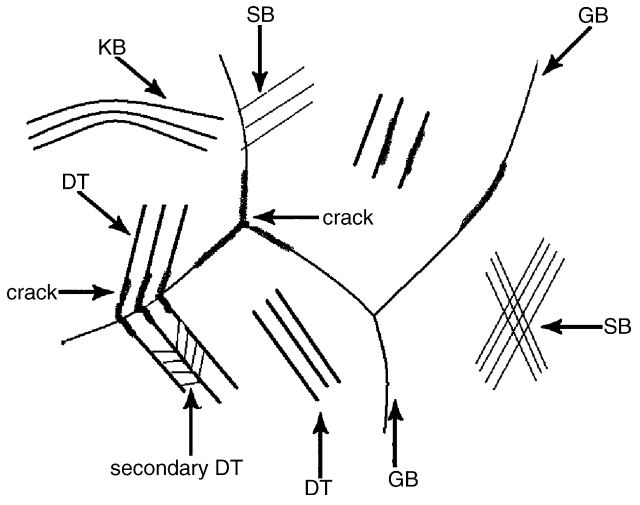

Fig. 12. Illustration of the micro-scale deformation and damage mechanisms of polycrystalline Zn under compression and cyclic compression–compression tests.

4. Conclusions

Based on the experimental results and discussion above, the following conclusions can be drawn:

(1) The deformation and damage mechanisms of commercially pure zinc under unidirectionally compressive tests are slightly distinctive at different compressive strains. The main deformation and damage mechanisms are twinning and secondary twinning, slipping, and cracking at grain boundaries and deformation twin boundaries. And grain boundaries can terminate twin boundary cracks.
(2) Compression–compression fatigue tests on the commercially pure zinc showed that the specimens displayed obvious cyclic hardening, and that the main damage mechanism is attributed to the combination of local cracks, deformation twins, secondary twins, slipping as well as kinking bands. Grain boundaries cannot terminate twin boundary cracks, and this is the main difference of damage mechanisms between unidirectional compression and cyclic compression–compression loadings.

Acknowledgements

The authors would like to thank D.R. Fang, F.F. Wu, W. Gao and H.H. Su for mechanical tests and SEM observations. This work was financially supported by the "Hundred of Talents Project" by the Chinese Academy of Sciences, the National Natural Science Foundation of China (NSFC) under grant nos. 50571104 and 50671023, and the National Outstanding Young Scientist Foundation for Z.F. Zhang under grant no. 50625103.

References

[1] M.H. Yoo, Metall. Trans. A 20 (1986) 1581.
[2] G.E. Dieter, Mechanical Metallurgy, McGraw-Hill, New York, 1976, p. 135.
[3] P.B. Price, Proc. R. Soc. A260 (1960) 251.
[4] N.E. Paton, W.A. Backoften, Metall. Trans. 1 (1970) 2389.
[5] X.L. Tan, H.C. Gu, S.F. Zhang, Mater. Sci. Eng. A189 (1994) 77.
[6] X.L. Tan, H.C. Gu, Z.G. Wang, Mater. Sci. Eng. A196 (1995) 45.
[7] X.L. Tan, H.C. Gu, Scripta Metall. Mater. 33 (1995) 77.
[8] X.L. Tan, H.C. Gu, Int. J. Fatigue 18 (1996) 329.
[9] X.L. Tan, H.C. Gu, N. Munroe, Scripta Mater. 36 (1997) 1383.
[10] Z.F. Zhang, H.C. Gu, X.L. Tan, J. Mater. Sci. Lett. 17 (1998) 211.
[11] Z.F. Zhang, H.C. Gu, X.L. Tan, Mater. Sci. Eng. A252 (1998) 85.
[12] X.L. Tan, H.C. Gu, C. Laird, Metall. Mater. Trans. 29A (1998) 507.
[13] X.L. Tan, H. Guo, H.C. Gu, Metall. Mater. Trans. 29A (1998) 513.
[14] C.Y. Hyun, H.K. Kim, Scripta Mater. 54 (2006) 1745.

[15] I. Kim, J. Kim, D.H. Shin, C.S. Lee, S.K. Hwang, Mater. Sci. Eng. A342 (2003) 302.
[16] H. Francillette, B. Bacroix, M. Gasperini, Mater. Sci. Eng. A234 (1997) 974.
[17] J.F. Binqert, T.A. Mason, G.C. Kaschner, Metall. Mater. Trans. 33A (1992) 955.
[18] P. Lukac, Z. Trojanova, A. Svobodova, Czech. J. Phys. B31 (1981) 163.
[19] R.L. Bell, R.W. Cahn, Proc. R. Soc. A239 (1957) 494.
[20] J.P. Toronchuk, Mater. Evol. 10 (1977) 51.
[21] F. Chmelik, Z. Trojanova, P. Lukac, J. Mater. Sci. Lett. 12 (1993) 1086.
[22] F. Chmelik, Z. Trojanova, P. Lukac, J. Mater. Sci. Lett. 12 (1993) 1166.
[23] C. Carl, X. Zhang, H. Wang, R.O. Scattergood, J. Narayan, A.V. Sergueeva, A.K. Mukherjee, Acta Mater. 50 (2002) 4823.
[24] J.J. Gilman, Trans. Am. Inst. Min. (Metall.) Eng. 206 (1956) 998.